NIH Public Access

Author Manuscript

IEEE Photonics Technol Lett. Author manuscript; available in PMC 2011 March 16.

Published in final edited form as:

IEEE Photonics Technol Lett. 2010 July 12; 22(15): 1147–1149. doi:10.1109/LPT.2010.2051145.

NIH-PA Author Manuscript

NIH-PA Author Manuscript

NIH-PA Author Manuscript

Hollow ARROW Waveguides on Self-Aligned Pedestals for Improved Geometry and Transmission

Evan J. Lunt[Student Member, IEEE],
Department of Electrical and Computer Engineering, Brigham Young University, Provo, UT 84602 USA

Bin Wu,
School of Engineering, University of California Santa Cruz, Santa Cruz, CA 95064 USA

Jared M. Keeley,
Department of Electrical and Computer Engineering, Brigham Young University, Provo, UT 84602 USA

Philip Measor[Student Member, IEEE],
School of Engineering, University of California Santa Cruz, Santa Cruz, CA 95064 USA

Holger Schmidt[Senior Member, IEEE], and
School of Engineering, University of California Santa Cruz, Santa Cruz, CA 95064 USA

Aaron R. Hawkins[Senior Member, IEEE]
Department of Electrical and Computer Engineering, Brigham Young University, Provo, UT 84602 USA

Evan J. Lunt: van.lunt@gmail.com; Bin Wu: binwu@soe.ucsc.edu; Jared M. Keeley: jamakee@hotmail.com; Philip Measor: pmeasor@soe.ucsc.edu; Holger Schmidt: hschmidt@soe.ucsc.edu; Aaron R. Hawkins: hawkins@ee.byu.edu

Abstract

Micrometer-sized hollow antiresonant reflecting optical waveguides on silicon substrates have been previously demonstrated with liquid and gas-filled cores. Previous designs have nonideal geometries, with nonuniform lateral layers around the hollow core, resulting in higher loss than could potentially be achieved. A new design and fabrication process has been developed involving hollow waveguide fabrication on a self-aligned pedestal (SAP) using anisotropic plasma etching. With the SAP structure, the hollow core is surrounded by uniform layers and a terminal layer of air on three sides, resulting in air-core waveguide loss of 1.54 cm^{-1} at 785 nm and high fabrication yield.

Index Terms

Fabrication; optical waveguides; plasma materials-processing applications

I. Introduction

Hollow optical waveguides enable waveguiding in low-index media and direct light interaction with a variety of nonsolid media. Many applications in biology, chemistry, and atomic physics can benefit from this capability. Two methods of realizing hollow waveguides are commonly used: index guiding and interference guiding. As with traditional

Color versions of one or more of the figures in this letter are available online at http://ieeexplore.ieee.org.

NIH-PA Author Manuscript NIH-PA Author Manuscript NIH-PA Author Manuscript

optical waveguides, index-guiding hollow waveguides rely on total internal reflection and require the cladding to have a lower refractive index than the core. Consequently, index-guiding hollow waveguides have been limited to liquid media ($n \approx 1.33$) and use low-index cladding materials such as nanoporous films [1] or Teflon AF [2]. Interference-guiding allows for waveguiding in both gas and liquid-filled cores, relying on optical interference to confine light to the low-index core. Some types of hollow waveguides created using interference-guiding are photonic crystals [3], Bragg waveguides [4], and antiresonant reflecting optical waveguides (ARROWs) [5], [6].

ARROW waveguides rely on one or more antiresonant layers surrounding a guiding core [7]. The thickness of each layer is chosen such that the layer functions as a reflecting Fabry–Pérot etalon, allowing for low-loss optical guiding along the core. We have developed ARROW waveguides with micrometer-sized hollow cores and have integrated hollow and traditional solid waveguides to form sensor platforms. These platforms have been used for many applications with both liquid and air-filled cores, including optical trapping [8], virus detection [9], and on-chip Rubidium spectroscopy [10].

Our ARROW waveguides are fabricated on Si substrates and use standard processing techniques, including plasma-enhanced chemical vapor deposition (PECVD), contact lithography, and sacrificial etching. Hollow ARROWs demonstrated in the past were fabricated on planar [5] or pre-etched substrates [11], and structures were nonideal for lowest loss. In this letter, we present a new fabrication method for hollow-core ARROWs, using a self-aligned pedestal (SAP) to create near-ideal hollow-core geometries with lower waveguide loss and high fabrication yield.

II. Low-Loss ARROW Design

The first hollow ARROWs were fabricated on a planar substrate, as shown in Fig. 1(a). While ARROWs are inherently leaky waveguides, this design is particularly leaky because horizontal layers extend laterally from the hollow core. Light leaks out of the sides of the hollow core and into these horizontal cladding layers, resulting in high loss. Also, the PECVD layers do not uniformly coat the rectangular waveguide core, and the top of the core is coated more thickly than the sides. This leads to a shadowing effect for film deposition on the sides of the core, with the vertical cladding layers slightly thinner at the bottom than at the top. These nonuniform lateral layers also contribute to higher loss.

One approach to increase light confinement and decrease loss in ARROWs is to surround the guiding core on three sides with a terminal layer of air [11]. To achieve this air-clad structure, we investigated a second ARROW design which consists of creating hollow waveguides on top of a pre-etched substrate, as depicted in Fig. 1(b). This air-clad structure increases light confinement in the core and results in lower loss than achieved with the first ARROW design. With this second design, it is necessary to create a pedestal on the substrate which is wider than the core to allow for alignment variations when the core is defined. In practice, any misalignment results in a noncentered core, which increases loss. The wider pedestal creates nonuniform layers on the sides of the core, which also increases loss. Another drawback with this structure is reduced fabrication yield, which occurs because of weakness in the films on the sides of the core where breakage can occur during sacrificial core removal.

Ideally, the hollow ARROW core would have uniform surrounding layers and a terminal layer of air on three sides. This third-generation ARROW design relies on an SAP to create the desired geometry. Since the width of the underlying pedestal is defined by the sacrificial

NIH-PA Author Manuscript

NIH-PA Author Manuscript

NIH-PA Author Manuscript

core, no alignment step is necessary. The uniform layers on the sides of the core would reduce loss and increase the strength of the structure, resulting in higher yield.

III. Fabrication

In order to fabricate SAP ARROWs, a process based on anisotropic plasma etching was chosen and is depicted in Fig. 2. The rest of the fabrication process is similar to that for ARROWs on planar substrates, based on PECVD and sacrificial etching [5]. First, layers of silicon dioxide (SiO_2) and silicon nitride (SiN) are deposited by PECVD on a Si substrate at 250 °C [see Fig. 2(a)]. These layers are deposited with controlled refractive indexes and precise thicknesses so that each layer satisfies the antiresonant condition [7]. Next, the SU-8 sacrificial layer is deposited and patterned into the core shape by photolithography. After this, the SAP is created by anisotropic plasma etching, using a Minilock Phantom III Reactive Ion Etcher (RIE) with an inductively coupled plasma (ICP) RF generator (Trion Technology). Selective etching is required so that the SU-8 core is not removed while etching through 1–1.5 μm of PECVD SiO_2 and SiN layers and 4–5 μm of the Si substrate to form the pedestal. We have developed separate etch recipes for etching the PECVD layers and the Si substrate, as shown in Table I. Etching of the PECVD layers is performed in a single etch step at an average rate of 170 nm/min. Etching of the Si substrate is performed with alternating sidewall passivation and etch steps, repeated many times, with an etch rate of about 18 nm/s.

The CHF_3 in the etching recipes provides sidewall passivation and increases the anisotropy of the etch. During etching, a fluorocarbon passivation film is deposited isotropically on the surface. Ion bombardment keeps horizontal surfaces clear of the film, while the film accumulates on and protects vertical surfaces. After etching is completed, the accumulated passivation film, commonly called post-etch residue, remains on the sides of the pedestal and the sacrificial core, and must be removed prior to deposition of the top antiresonant layers.

Various approaches have been used to remove this etch residue, including O_2 and H_2 plasmas, hydroxylamine, super-critical CO_2 ($SCCO_2$) [12], and radical anions [13]. We developed a cleaning procedure using a mixture of H_2O_2 and the resist remover RS-6 (Cyantek Corp.), which contains tetramethylammonium hydroxide (TMAH). To remove the etch residue, our samples are immersed in the mixture (1 : 10 50% H_2O_2 RS – 6) at 40 °C for 5 min and then rinsed in deionized water. This cleaning process is performed after the SiO_2–SiN etch and again after the Si etching and effectively removes the etch residue without damaging the SU-8 core.

Another common problem encountered with anisotropic etching is the formation of etch grass. This occurs when surface defects and contamination function as micromasks and lead to the formation of small pillars, known as grass, on the etched surface. This issue can be particularly severe in our SAP etching, as the PECVD layers contain many defects which can function as micromasks [14]. To remove this etch grass, we employ an isotropic Si etch at the end of the pedestal etching. This etch attacks the sides of the grass and etches away the Si base to the point that the grass collapses, so it can be later rinsed away.

After the pedestal etching is completed and the etch residue and grass are removed, the top antiresonant layers are deposited by PECVD [see Fig. 2(c)]. Finally, the ends of the sacrificial core are exposed, either by cleaving the wafer or by plasma etching, and the core is removed in a piranha etch (1 : 1 50% H_2O_2 : 98% H_2SO_4, 100 °C), completing the hollow waveguide, as depicted in Fig. 2(d).

NIH-PA Author Manuscript NIH-PA Author Manuscript NIH-PA Author Manuscript

Fig. 3 shows an SEM image of a completed hollow SAP ARROW with nearly ideal geometry. Compared to the second ARROW design [see Fig. 1(b)], we see that the layers on the sides of the core are uniform, which is expected to decrease waveguide loss and increase yield with SAP ARROWs.

IV. Experimental Results

In order to characterize the waveguide loss of this new structure, we created straight SAP ARROWs with cores 5.8 μm tall and 9, 12, and 15 μm wide. The dielectric layer thicknesses were optimized for air cores at 785 nm, and the target thicknesses were (starting from the substrate—all values in nanometers): SiO_2–**SiN**–SiO_2–**SiN**–SiO_2–**SiN –** core – **SiN**–SiO_2–**SiN**–SiO_2–**SiN**–SiO_2 (150/**110**/165/**100**/190/**90** – 5800– **61**/324/**94**/284/**234**/4010). These layer thicknesses differ from those predicted by the antiresonant condition for one-dimensional confinement (SiN, $n = 2.05 : 110$ nm, SiO_2, $n = 1.46 : 184$ nm), since this design has been optimized for this particular structure and additional fabrication considerations (see [11]). Fabrication yield with the SAP ARROWs was very good, with over 90% of channels intact for waveguides up to 15 mm long for all three widths.

Previously, the lowest loss for air-core hollow ARROWs at 785 nm was achieved using the pre-etched pedestal design and was 2.6 cm^{-1} for a 5.8×15 μm hollow core [11]. To characterize the air-core loss for SAP ARROWs, the standard cutback method was used with light at 785 nm. Average losses were determined to be 3.31, 2.19, and 1.54 cm^{-1} for 9-, 12-, and 15-μm-wide waveguides, respectively. Losses for the two designs are shown in Fig. 4, and we see that losses for air-cores at 785 nm are greatly reduced for the SAP ARROWs for all three waveguide widths.

In conclusion, we have presented a new SAP design and fabrication method for hollow ARROW waveguides that produces nearly ideal hollow-core geometries. Air-core devices fabricated with this new process have record-low losses at 785 nm and over 90% fabrication yield. For our current integrated ARROW platforms with 4-mm-long hollow waveguides, light transmission should be improved by more than two times with the SAP ARROWs, which will increase sensitivity and performance of ARROW-based sensing and spectroscopy devices.

Acknowledgments

This work was supported by the NIH/NIBIB (Grant R01-EB006097), by the NSF (Grant ECS-0528714 and Grant ECS-0528730), and by the W. M. Keck Center for Nanoscale Optofluidics at UCSC.

References

1. Korampally V, Mukherjee S, Hossain M, Manor R, Yun M, Gangopadhyay K, Polo-Parada L, Gangopadhyay S. Development of a miniaturized liquid core waveguide system with nanoporous dielectric cladding—A potential biosensing platform. IEEE Sensors J. Dec; 2009 9(12):1711–1718.
2. Datta A, Eom IY, Dhar A, Kuban P, Manor R, Ahmad I, Gangopadhyay S, Dallas T, Holtz M, Temkin H, Dasgupta P. Micro-fabrication and characterization of Teflon AF-coated liquid core waveguide channels in silicon. IEEE Sensors J. Dec; 2003 3(6):788–795.
3. Abouraddy AF, Bayindir M, Benoit G, Hart SD, Kuriki K, Orf N, Shapira O, Sorin F, Temelkuran B, Fink Y. Towards multimaterial multifunctional fibres that see, hear, sense and communicate. Nat Mater. May; 2007 6(5):336–347. [PubMed: 17471274]
4. Ponnampalam N, DeCorby RG. Self-assembled hollow waveguides with hybrid metal-dielectric Bragg claddings. Opt Express. 2007; 15(20):12595–12604. [PubMed: 19550527]
5. Yin D, Schmidt H, Barber J, Hawkins A. Integrated ARROW waveguides with hollow cores. Opt Express. 2004; 12(12):2710–2715. [PubMed: 19475112]

6. Bernini R, De Nuccio E, Minardo A, Zeni L, Sarro P. 2-D MMI devices based on integrated hollow ARROW waveguides. IEEE J Sel Topics Quantum Electron. Mar./Apr; 2007 13(2):194–201.
7. Duguay MA, Kokubun Y, Koch TL, Pfeiffer L. Antiresonant reflecting optical waveguides in SiO_2 – Si multilayer structures. Appl Phys Let. 1986; 49(1):13–15.
8. Kühn S, Measor P, Lunt EJ, Phillips BS, Deamer DW, Hawkins AR, Schmidt H. Loss-based optical trap for on-chip particle analysis. Lab Chip. 2009; 9(15):2212–2216. [PubMed: 19606298]
9. Rudenko M, Kuhn S, Lunt E, Deamer D, Hawkins A, Schmidt H. Ultrasensitive *Qβ* phage analysis using fluorescence correlation spectroscopy on an optofluidic chip. Biosens Bioelectron. 2009; 24(11):3258–3263. [PubMed: 19443207]
10. Wu B, Hulbert J, Hawkins A, Schmidt H. Planar hollow-core waveguide technology for atomic spectroscopy and quantum interference in alkali vapors. J Lightw Technol. Dec 1; 2008 26(23): 3727–3733.
11. Yin D, Barber J, Hawkins A, Schmidt H. Waveguide loss optimization in hollow-core ARROW waveguides. Opt Express. 2005; 13(23):9331–9336. [PubMed: 19503133]
12. Myneni S, Hess DW. Post-plasma-etch residue removal using CO_2-based fluids. J Electrochem Soc. 2003; 150(12):G744–G750.
13. Timmons CL, Hess DW. Photoresist and fluorocarbon post-plasma etch residue removal using electrochemically generated radical anions. J Electrochem Soc. 2008; 155(10):H771–H777.
14. Lunt EJ, Phillips BS, Keeley JM, Hawkins AR, Measor P, Wu B, Schmidt H. Hollow ARROW waveguides on self-aligned pedestals for high-sensitivity optical sensing. Proc SPIE. 2010; 7591:759109.

NIH-PA Author Manuscript
NIH-PA Author Manuscript
NIH-PA Author Manuscript

NIH-PA Author Manuscript

NIH-PA Author Manuscript

NIH-PA Author Manuscript

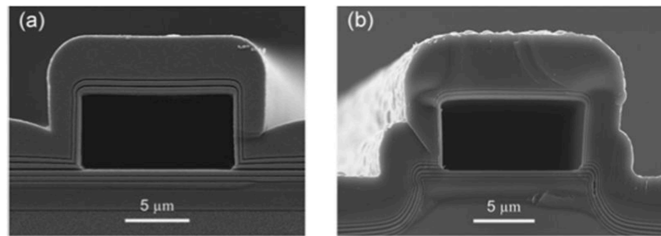

Fig. 1.

ARROW hollow waveguide designs: (a) First design on a planar substrate. (b) Second design on a pre-etched substrate. (Light gray: SiO_2; dark gray: SiN).

NIH-PA Author Manuscript

NIH-PA Author Manuscript

NIH-PA Author Manuscript

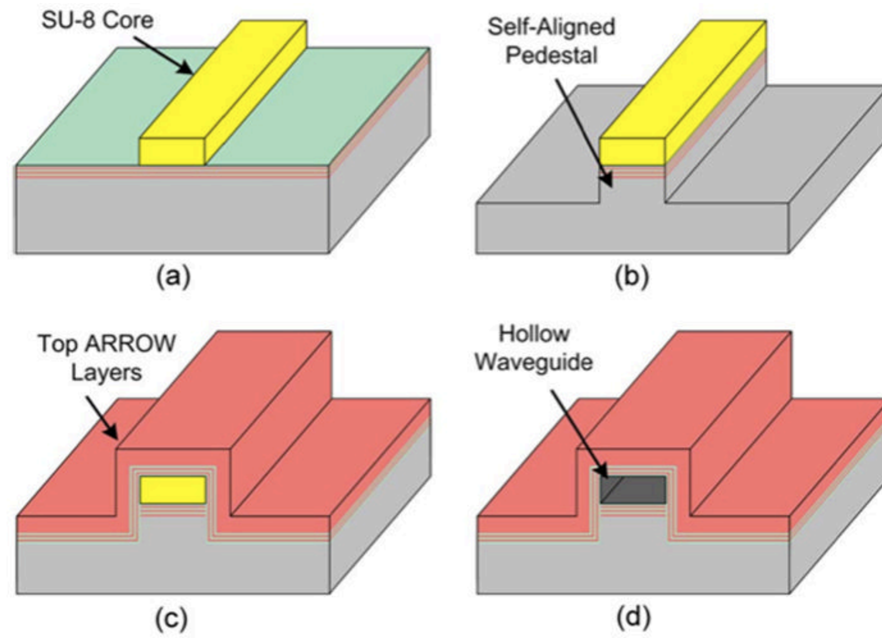

Fig. 2.

Cross-sectional view of SAP ARROW fabrication: (a) Bottom PECVD antiresonant layers and sacrificial SU-8 core deposited. (b) SAP etched. (c) Top PECVD antiresonant layers deposited. (d) Sacrificial core exposed and removed in a piranha etch, completing the hollow waveguide.

NIH-PA Author Manuscript
NIH-PA Author Manuscript
NIH-PA Author Manuscript

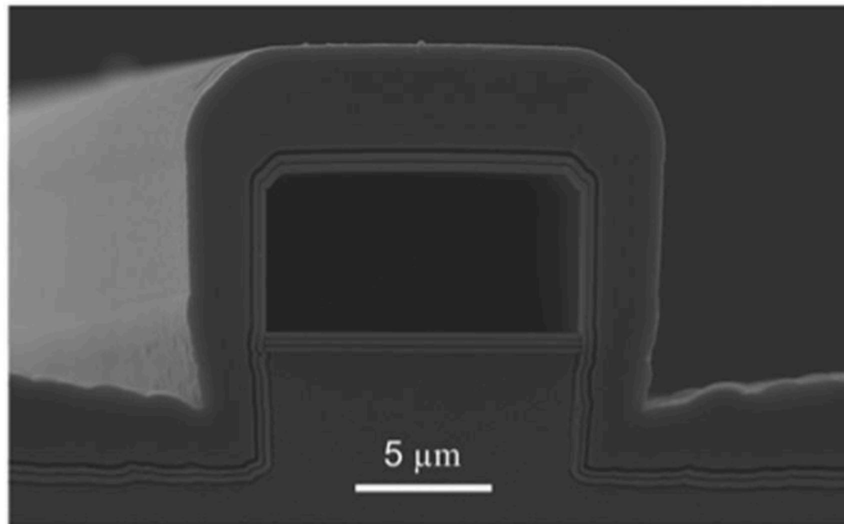

Fig. 3.
SEM image of a completed hollow ARROW on an SAP. (Light gray: SiO_2; dark gray: SiN).

NIH-PA Author Manuscript

NIH-PA Author Manuscript

NIH-PA Author Manuscript

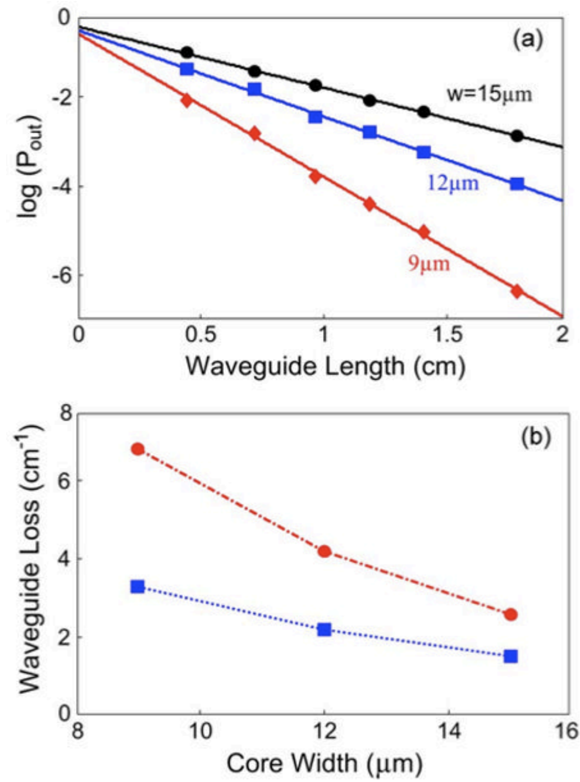

Fig. 4.

(a) Transmitted power versus SAP waveguide length with air-filled cores at 785 nm (symbols: experiment, lines: exponential fits). (b) Experimental hollow waveguide loss with air-filled cores at 785 nm for different core widths (height = 5.8 μm; circles: ARROWs on pre-etched substrates, squares: ARROWs on SAPs.

NIH-PA Author Manuscript
NIH-PA Author Manuscript
NIH-PA Author Manuscript

Table I

SAP Etching Recipes

Recipe	ICP (W)	RIE (W)	Pressure (mTorr)	Gases (sccm)		
				CHF_3	O_2	SF_6
SiO_2 and SiN	350	70	18	125	9	0
Si Passivation	550	0	120	75	0	0
Si Etch	550	60	35	30	0	20
Isotropic Si Etch	0	200	150	0	0	52